scientific reports

Check for updates

OPEN

ANO1 channels are expressed in mouse urethral smooth muscle but do not contribute to agonist or neurally evoked contractions

Neha Gupta[1], Salah A. Baker[2], Kenton M. Sanders[2], Kaneez E. Rabab[1], Denzel KF. Thean[1], Tuleen Alkawadri[1], Caoimhin S. Griffin[1], Gerard P. Sergeant[1], Mark A. Hollywood[1], Keith D. Thornbury[1] & Bernard T. Drumm[1]✉

Anoctamin-1 Ca^{2+}-activated Cl^- channels (ANO1) are proposed to modulate contractility of urethra smooth muscle cells (USMC), but their cellular expression and contribution to agonist/neural evoked activity is unclear. ANO1 is implicated as a potential target to treat incontinence, thus this is an important issue to resolve. We sought to clarify roles of ANO1 in contractility of mouse USMC. We found expression of *Ano1* transcripts in murine urethra, with no difference between male and females. Immunolabelling revealed ANO1 was expressed in USMC and not in specialized populations of interstitial cells (c-kit$^+$ interstitial of Cajal-like cells (ICC-LC) and PDGFRα$^+$ cells). However, a specific ANO1 channel inhibitor, Ani9, failed to affect urethral contractions elicited by phenylephrine, arginine vasopressin or electrical field stimulation of intrinsic nerves. $CaCC_{inh}$A01 also failed to affect urethral contractions. In addition, Ani9 had no effect on Ca^{2+} signals generated by USMC in situ. In contrast, Ani9 effectively reduced spontaneous contractions and Ca^{2+} signals of mouse proximal colon. In addition, Ani9 inhibited ANO1 currents recorded in HEK 293 cells, at concentrations 30 times less than those used in organ bath experiments. Our data suggest that despite expression of ANO1 in USMC, these channels do not contribute to basal Ca^{2+} signalling, or agonist and neurally-evoked contractions in murine urethra.

Keywords Urethra, Ca^{2+}-activated-Cl^-, Smooth muscle, Incontinence, Ani9, ANO1

Anoctamin-1 Ca^{2+}-activated Cl^- channels (ANO1), are expressed in multiple smooth muscle organs[1]. In smooth muscle cells (SMCs), Cl^- is actively accumulated due to Cl^-/HCO_3^- exchangers and Na^+, K^+, Cl^- cotransporters[2]. This results in a Cl^- equilibrium potential (E_{Cl}, estimated between − 30 to -20mV[3]) positive to resting membrane potential[4]. Thus, activation of ANO1 leads to Cl^- efflux and depolarization[5], which can modulate SMC excitability by increasing opening of voltage-dependent Ca^{2+} channels required for excitation-contraction coupling[2,6].

In the lower urinary tract (LUT), ANO1 is implicated in regulating urethral tone, contributing to urinary continence[7–9]. During bladder filling, urethral SMCs (USMC) contract, summating as myogenic tone to occlude the urethra and prevent bladder leakage[10,11]. Urethral smooth muscle (USM) tone is myogenic but can be enhanced by adrenergic stimulation via noradrenaline[12,13] and relaxed by nitric oxide during voiding[14,15]. Ca^{2+}-activated-Cl^- channel antagonists, such as niflumic acid, inhibited electrical 'slow waves' and depolarizations in rabbit and guinea-pig urethra[16,17]. Ca^{2+}-activated Cl^- channel antagonists, 9-AC and niflumic acid, reduced adrenergic evoked contractions of rabbit USM[18], and phenylephrine-induced contractions of mouse and sheep USM[9]. More specific ANO1 channel antagonists, such as $T16_{inh}$A01, reduced rabbit USM tone and contractions evoked by nerve stimulation[8].

Cellular expression of ANO1 in urethra may differ between species. ANO1 mRNA expression is enriched in vimentin$^+$ interstitial cells in rabbit[8], and their spontaneous electrical activity was inhibited by broad spectrum Ca^{2+}-activated-Cl^- channel antagonists[18–20] and ANO1 antagonists[8]. Urethral interstitial cells label with antibodies against c-kit (biomarker for interstitial cells of Cajal (ICC) in the GI tract, which exclusively express ANO1[21,22]) in some studies[23,24]. We will collectively refer to these cells as interstitial cell of Cajal-like cells (ICC-

[1]Smooth Muscle Research Centre, Department of Life & Health Science, Dundalk Institute of Technology, Dundalk, Co. Louth, Ireland. [2]Department of Physiology & Cell Biology, University of Nevada, Reno School of Medicine, Reno, NV, USA. ✉email: bernard.drumm@dkit.ie

LC), due to morphological and proposed functional commonalities with c-kit$^+$ ICC in the gut[25]. In contrast to rabbits, ANO1 immunoreactivity in mouse, rat and sheep is confined to USMC, with no detection of ANO1 in ICC-LC[9].

Most evidence for a role of ANO1 in urethral function derives from pharmacological agents such as niflumic acid, DIDS, MONNA, $CaCC_{inh}A01$ or $T16_{inh}A01$. These agents can exert off-target effects including inhibition of voltage-dependent Ca^{2+} channels[26] or activation / block of Ca^{2+} release channels on sarcoplasmic reticulum (SR) membranes[27,28]. Thus, studies in which the effects of these agents were tested on muscle contractions could be problematic. Therefore, in the current study we revisited the question of whether ANO1 is involved in contractions elicited by exogenous agonist or stimulation of excitatory neurons in mouse urethra.

We characterized expression of *Ano1* transcripts in urethra muscles using quantitative PCR and expression of ANO1 protein in USMC and different populations of interstitial cells with immunohistochemistry. In contractile and Ca^{2+} imaging studies, we tested Ani9, a specific antagonist of ANO1 channels[29] that lacks off-target effects on voltage-dependent Ca^{2+} current[30] and SR Ca^{2+} release in SMCs[27,28] at concentrations effective in blocking ANO1.

Methods

Ethical approval

This study adhered to the guidelines set forth in the National Institutes of Health (NIH) Guide for the Care and Use of Laboratory Animals. The Institutional Animal Use and Care Committee (IACUC) at the University of Nevada, Reno (UNR) approved of animal use and protocols at UNR, and the Animal Ethics Committee at Dundalk Institute of Technology (DkIT) approved all animal use and protocols conducted at DkIT. All protocols align with the ARRIVE guidelines.

Animals

Wild type (WT) C57BL/6 mice and Acta2-GCaMP8.1 mice were purchased from the Jackson Laboratory (Bar Harbor, ME, USA) and bred in house. $GCaMP6f^{lox/+}$ mice (B6; 129 S-Gt(ROSA)$^{26Sortm95.1(CAG–GCaMP6f)Hze}$/J) were purchased from the Jackson Laboratory (Bar Harbor, ME, USA) and were crossed with Kit-iCre expressing mice (Kit-tm1cre/ER^{T2}Dsa, gifted from Dr. Dieter Saur of the Technical University Munich, Germany) to generate Kit-GCaMP6f mice for conditional expression of GCaMP6f in c-Kit$^+$ cells as described previously[31]. Induction of GCaMP6f in Kit-GCaMP6f was performed as previously described[31–34]. Briefly, Kit-GCaMP6f mice were injected with tamoxifen between 6 and 8 weeks of age to induce expression of GCaMP6f in Kit-expressing cells. Tamoxifen, obtained from Sigma, was dissolved in ethanol (Pharmco-Aaper 200 proof, absolute, anhydrous) at a concentration of 0.1 mg μL^{-1} and vortexed for 20 min. Safflower oil (generic) was added to create a final volume of 20 mg/ml, and the solution was sonicated for 30 min. The GCaMP mice were injected intraperitoneally with the tamoxifen solution (2 mg total tamoxifen) for 3 consecutive days. Ten days after the initial tamoxifen injection, the mice were genotyped to confirm Cre-mediated GCaMP production. Upon confirmation of GCaMP expression, the mice were used for experiments.

Tissue preparation

Mice were anesthetized with isoflurane (99.9% Baxter, Deerfield, IL, USA) and sacrificed by cervical dislocation prior to being used in experiments. Their abdomens were opened, and their bladders and proximal urethras were removed and placed in Krebs-Ringer bicarbonate solution (KRB). The urethras were then opened along a longitudinal incision, and the urothelium was carefully removed through sharp dissection. The urothelium was auto fluorescent and thus was removed (along with underlying lamina propria) to prevent capture of contaminating signal during imaging experiments. Colonic tissues were removed from mice and the proximal region was used for experimentation. Colons were opened along a longitudinal axis and contents were washed away with KRB solution. Mucosal and sub-mucosal layers were removed with fine forceps. The penis was removed from the pelvic bone and dissected to expose the corpus cavernosum, which was used for immunocytochemistry experiments along with urinary bladder. Bladders were opened with longitudinal incision and urothelium were peeled off before cell dispersal.

Calcium imaging

Acta2-GCaMP8.1 mice urethral muscle and colonic tissues were immobilized in a 5 ml, 60 mm diameter Sylgard-coated dish using fine tungsten pins as outlined previously[25]. Tissues were placed in dishes with luminal side facing upwards. Tissues were continuously supplied with a warmed KRB solution (37°C) for 1 h before experiments began to allow for equilibration. Imaging experiments were conducted with an Olympus BX51WI microscope, equipped with a 40x Olympus FL N objective and a FITC HQ series fluorescence filter cube. The filter cube had a dichroic with a 510 nm barrier filter and a 535 nm filter. GCaMP was excited at a wavelength of 488 nm. Images were acquired at 33 frames per sec using a high-speed EMCCD camera (Andor iXon-Ultra 897 EMCCD Camera; ANDOR Technology, Belfast, UK) and Andor IQ software. For pharmacological tests, a 20–30 s control period was recorded, followed by the addition of the drug to the KRB solution for 15 min to allow for full tissue penetration. The effects of the drug were then recorded for an additional 20–30 s.

Analysis of Ca^{2+} signals

Analysis of Ca^{2+} signals was performed as previously described[35]. Movies of in situ Ca^{2+} activity were converted to a stack of TIFF (tagged image file format) images and imported into ImageJ (version1.54e, National Institutes of Health, MD, USA, http://rsbweb.nih.gov/ij). Spatio-temporal maps (STMs) of Ca^{2+} activity were generated by drawing a single pixel line along the mid axis of the cell and the 'reslice' function in ImageJ was used to create a STM which was then calibrated for distance and time. The basal Ca^{2+} fluorescence was acquired from

regions of the cell displaying the most uniform and least intense fluorescence (F_0). F_0 was calculated by averaging the fluorescence in these regions, during periods of quiescence for a minimum of 2 s. The fluorescence value throughout the cell was then divided by the calculated F_0 value to calibrate the STM for amplitude of Ca^{2+} events as $\Delta F/F_0$. Events with amplitude > 20% of the maximum amplitude event were considered for analysis. Ca^{2+} event frequency was expressed as the number of events fired per cell per minute (min^{-1}). The amplitude of Ca^{2+} events was expressed as $\Delta F/F_0$, the duration of Ca^{2+} events was expressed as full duration at half-maximum amplitude (FDHM) and the spatial spread of Ca^{2+} events was expressed as micrometers (μm) of cell propagated per Ca^{2+} event.

Immunohistochemistry

Immunolabeling of urethral muscle was performed as previously described[25]. Each ring of Kit-GCaMP6f and WT mouse proximal urethra was longitudinally cut and pinned at all four corners with tungsten wire onto a Sylgard-based dish and the urothelium was removed by sharp dissection. The tissue was then fixed in 4% paraformaldehyde (PFA) for 20–30 min at room temperature. Tissues were then washed in phosphate saline buffer (PBS, 0.01 M, pH 7.2) for 5 h, with PBS changed every hour. Tissues were permeabilized with 0.5% Triton X-100 (Sigma life science) for 1 h before repeated washes with PBS (3x). Tissues were subsequently incubated in donkey serum (10%; 2 h at RT) to reduce non-specific antibody binding. Tissues were incubated in primary antibodies (see Table 1) for 48 h at 4 °C followed by washing with PBS for 5 h. Then, tissues were incubated in secondary antibodies (Jackson Immunoresearch laboratories) diluted in PBS (1:1000): Alexa Fluor anti-chicken 488, Alexa Fluor anti-goat 488 and Alexa Fluor anti-rabbit 594 for 1 h at room temperature followed by repeated PBS washes for 5 h. Tissues were mounted on slides using Vectashield mounting media. The mount was then imaged on the Leica Stellaris 5 confocal system with a DMi8 inverted automated fluorescence microscope. Leica Application Suite X (LAS X) software was used to capture Z-stack images of various depths of tissue at objective of 20x and 40x. The final images were constructed using the LAS X software (version 5.1.0.25593) and converted to TIFF files.

Immunocytochemistry

SMC were dispersed from WT mouse urethra (both male and female), bladder and corpus cavernosum as outlined previously[30]. After dispersal, cells were adhered to coverslips coated with poly-l-lysine on ice. Cells were then fixed with 2% PFA for 30 min and washed three times with 1% PBS. Cells were then permeabilized with 0.1% Triton X (Sigma life science) for 10 min and washed thrice with 1% PBS. Blocking was performed with 50% SEA block (Thermo Fisher Scientific). The cells were co-stained with primary antibodies (see Table 1) overnight at 4^0 C. The cells were washed with 20% SEA block followed by incubation with secondary antibodies, Alexa Fluor donkey anti-mouse 555 (1:1000, life technologies) and Alexa Fluor goat anti-rabbit 488 (1:1000, invitrogen, Thermo Fisher Scientific) for 2 h. The cells were then washed and mounted on slides using Vectashield mounting media. The secondary antibody only controls were also performed similarly with no primary antibody staining. The mounted cells were then imaged on Axioskop 2 LSM 510 Meta confocal microscope (Zeiss, Germany) using a 20X objective. Confocal micrographs were generated from z-series scans taken at 0.5 μm depth interval. The final images were constructed using Fiji by Image J (version1.54f, National Institutes of Health, MD, USA, http://rsbweb.nih.gov/ij).

RNA extraction and quantitative polymerase chain reaction

Male and female mouse urethras were collected and pooled into three groups or biological replicates (6 urethras per biological replicate, $N = 3$, $n = 18$) for each sex prior to RNA extraction. Additionally, proximal colons were collected and used as a positive test control ($N = 3$, $n = 3$). Total RNA was isolated from male and female urethra and proximal colon using the Trizol method (Invitrogen). RNA samples were DNase treated (DNase 1, Invitrogen) to remove any contaminating genomic DNA. Equal concentration of DNase treated RNA was taken from each sample for cDNA synthesis. First-strand cDNA was prepared from RNA using Superscript II Reverse Transcriptase (Invitrogen). 200 μg/μl random hexamers were used to prepare cDNA. Real-time quantitative PCR (qPCR) was performed using the SYBR Green PCR Master Mix (Applied Biosystems). The qPCR reaction was performed in triplicates with three biological replicates of male and female urethras and proximal colons with PCR primers listed in Table 2. β-actin was used as an endogenous reference gene for sample normalization. The fold change expression ($2^{-\Delta\Delta CT}$) was calculated by taking proximal colon as a positive control.

Isometric tension recordings

Intact urethral rings, dissected from the bladder of wildtype mice were mounted in 14 ml water jacketed (37ºC) organ baths for tension recordings as previously described[36,37]. Organ baths were filled with KRB solution

Primary antibody	Host	Dilutions	Source
Anti-GFP	Chicken polyclonal	1:500	GFP-1010, Aves Labs
PDGFRα	Goat polyclonal	1:200	AF1062, R and D Systems
ANO1	Rabbit polyclonal	1:200	ab53212, Abcam
ANO1	Rabbit polyclonal	1:100	ACL-011, Alomone labs
Smooth muscle α-actin	Mouse monoclonal	1:100	M0851, Dako, Agilent

Table 1. Primary antibodies used in this current study.

Gene name	Sequence	Accession no.
Ano1-F	TAACCCTGCCACCGTCTTCT	NM_178642
Ano1-R	ATGATCCTTGACAGCTTCCTCC	
β– *actin-F*	CTAGGCACCAGGGTGTG	NM_007393.3
β– *actin-R*	GTGAGCAGCACAGGGT	

Table 2. List of gene primers utilized in the current study.

which was continually oxygenated throughout experimentation via an adjustable sparger at the base of the bath. Urethral rings were adjusted to an initial tension of 2 mN and left to equilibrate for 1 h prior to experimentation. Isometric contractions were recorded and analyzed using LabScribe software (WPI, version 4.34). Electrical field stimulation (EFS) of transmural nerves in urethral rings was carried out via two parallel platinum electrode wires placed either side of the tissue. EFS (pulse width of 0.3 ms) was applied with a MultiStim system-D330 stimulator (Digitimeter Ltd, England) at r 1, 2, 5, 10,20 Hz for durations of 30 s with 2 min between stimulations. These neurogenic urethral contractions evoked by EFS were analyzed by measuring the difference between the resting baseline immediately prior to onset of EFS (level of basal tone in the urethral ring before EFS was applied) and the peak of contractions during the EFS stimulus and were expressed as contraction amplitude (mN). All EFS experiments were performed in the presence of the neuronal nitric oxide synthase inhibitor Nω-nitro-L-arginine (L-NNA; 100 μM) to examine purely excitatory responses.

Patch-clamp recording on cultured HEK cells

Electrophysiological recordings were conducted on individual HEK cells 24–48 h after transfection with plasmid DNA encoding human ANO1 channels. All experiments were performed at room temperature. Patch pipettes were prepared from thin-walled borosilicate glass (1.5 mm outer diameter × 1.17 mm inner diameter; Clark Medical Instruments) and pulled to achieve a tip diameter of approximately 1–1.5 μm with a resistance of 2–5 MΩ. Voltage-clamp protocols were applied using an Axopatch 200 A amplifier (Axon Instruments) connected to a Digidata 1322 A AD/DA converter (Axon Instruments), controlled via a computer running pClamp software (Axon Instruments). Data were sampled at a rate of 10 kHz and filtered at 2 kHz. Series resistance was not compensated for, with estimated errors of less than 20 mV. During the recordings, HEK cells in the dish were continuously superfused with Hank's solution (composition detailed below). The pipette solution used to record whole-cell currents contained 100 nM Ca^{2+} (composition also described below). A close delivery system, consisting of a pipette with a tip diameter of ~ 200 μm positioned approximately 300 μm from the cell, provided continuous superfusion of Hank's solution over the cell under study. This system could be rapidly switched (with a dead-space time of approximately 5 s) to a solution containing Ani9 (100 nM). Ani9 was dissolved in Hank's solution to achieve the desired experimental concentration. Recordings were made using the whole-cell patch-clamp configuration[38]. To generate current-voltage (I-V) relationships, cells were held at a membrane potential of -60 mV, and whole-cell currents were recorded during voltage steps ranging from − 100 mV to + 120 mV, in increments of 20 mV. Tail currents were measured by stepping the membrane potential to -80 mV after each test potential. Leak currents were determined at the holding potential of -60 mV in the absence of any drug and were subtracted digitally.

Drugs and solutions

Tissues were perfused with KRB containing (mmol l^{-1}): NaCl, 120.35; KCl, 5.9; $NaHCO_3$, 15.5; NaH_2PO_4, 1.2; $MgCl_2$, 1.2; $CaCl_2$, 2.5; and glucose, 11.5. KRB was bubbled with a mixture of 95% O_2 – 5% CO_2 and warmed to 37 ± 0.2 °C.

HEK cells were super fused in Hank's solution containing (mmol l^{-1}): NaCl (140), KCl (5.36), Glucose (10), Sucrose (2.9), $NaHCO_3$ (4.17), KH_2PO_4 (0.44), Na_2HPO_4 (0.33), $MgCl_2.6H_2O$ (1.8), $CaCl_2.2H_2O$ (1.8), $MgSO_4.7H_2O$ (0.4), HEPES (10). pH adjusted to 7.4 with 3 M NaOH.

100 nM Ca^{2+} solution (pipette solution used in patch clamp recordings): NaCl (135), HEPES (10) and EGTA (10) Add 369.7 μl of 1 M $CaCl_2$ for 100 ml of 100 nM Ca^{2+} solution. pH adjusted to 7.2 with NaOH.

Nifedipine, niflumic acid, phenylephrine, 2-APB and L-NNA were purchased from Sigma-Aldrich (St Louis, MO, USA). TTX was purchased from Alomone labs. Ani9 and $CaCC_{inh}A01$ were purchased from Tocris Biosciences (Ellisville, MO, USA). All drugs were dissolved in the manufacturer-recommended solvent and then diluted into KRB solution for use in experiments.

Statistical analysis

Data are represented as mean ± standard error of the mean (SEM). Control data was tested for normality using a Shapiro-Wilk analysis, after which paired experiments with two datasets were analyzed using student's t-test (normal) or Wilcoxon's matched pairs signed rank test (non-normal). ANOVA with a Bonferroni post-hoc test was used to analyze data consisting of more than two datasets. In all statistical analyses, $P < 0.05$ was taken as significant. When describing data, n refers to the number of animals used in that dataset while c refers to the number of cells analyzed in that same data set. In qPCR experiments, 'n' refers to the number of biological replicates.

Results

ANO1 expression in urethral tissues

In an initial series of experiments, we firstly evaluated expression of *Ano1* genes and ANO1 protein in mouse urethra, and specifically its cellular expression pattern. In qPCR experiments, fold change expression of *Ano1* transcript relative to the colon (normalized to the housekeeping gene β-*actin*) in male and female urethras was 2.9 ± 0.3 ($n = 3$, Fig. 1A, $P = 0.03$) and 2.9 ± 0.4 ($n = 3$, Fig. 1A, $P = 0.03$) higher respectively. No statistical difference in *Ano1* expression was observed between male and female urethral tissues (Fig. 1A, $P > 0.99$).

Ca^{2+}-activated-Cl^{-} channels have been most extensively characterized in urethral tissues from rabbit, where ANO1 expression is mostly confined to ICC-LC[8]. Recently, we demonstrated that using anti-GFP antibodies was an effective means of visualizing ICC-LC from KitGCaMP6f mice (see Methods) with immunohistochemistry[25]. In the current study, antibodies against GFP in KitGCaMP6f mice labelled a population of elongated c-kit^{+} interstitial cells, which we refer to as ICC-LC (Fig. 1B). However, there was a lack of co-immunolabelling with ICC-LC and ANO1 antibodies in these same tissues, instead ANO1 antibodies appeared to label underlying USMC bundles (Fig. 1B, $n = 5$). In upper urinary and male reproductive tracts, ANO1 expression is localized within PDGFRα^{+} interstitial cells[39,40]. To test if such cells expressed ANO1 in the urethra, we co-incubated WT urethral muscle preparations with antibodies against PDGFRα and ANO1. PDGFRα^{+} cells were abundant in urethral tissues (Fig. 1C), however no evidence of co-labelling with ANO1 was observed, and ANO1 appeared once again to be confined to USMC bundles (Fig. 1C, $n = 3$).

Immunocytochemical staining was performed on male and female USMC with smooth muscle α-actin and ANO1 antibodies to confirm cellular ANO1 expression in single USMCs. In accordance with the immunohistochemical data above, we found that isolated USMC from both male and female tissues were readily labelled with antibodies against α-actin, and ANO1 (Fig. 2A&B, $n = 3$). Negative controls for cells lacking ANO1 (bladder SMC) and positive controls for cells previously demonstrated to express ANO1 (corpus cavernosum SMC) were also taken for validating immunocytochemistry antibodies as previously described[30]. Whereas corpus cavernosum SMC showed clear ANO1 expression colocalized with α-actin (Fig. 2C, $n = 3$), ANO1 expression was not detected in bladder SMCs, as it did not colocalize with α-actin expression (Fig. 2D, $n = 3$).

Effects of ANO1 Inhibition on urethral contractions

We next sought to determine how ANO1 inhibition affected urethral contractions. To do this, we initially conducted isometric tension recordings of USM rings of male WT mice (see Methods). Tissues were precontracted with an α1-adrenoreceptor agonist (phenylephrine, PE). Specifically, we performed PE dose-response curves ranging from 30 nM to 30 μM, applied for 10 min per concentration ($n = 6$, Fig. 3A). As PE concentration increased beyond 300 nM, evoked contractions developed a biphasic nature, consisting of an initial peak, followed by a partial decline and sustained contraction (Fig. 3A). In many instances, the amplitude of the initial peak and rate of subsequent decline increased as PE concentration increased. These characteristics could be variable between tissues, with some responses consisting mostly of sustained contractions, without obvious initial peaks. To analyse these traces and encompass the entire contraction, regardless of variability, we quantified PE responses as area under the curve (AUC; mN.s). We found that increased PE concentrations reliably increased AUC in a concentration-dependent manner. At concentrations of 100 nM PE, sustained contractions, averaging 34.3 ± 12.2 mN.s (AUC) were observed, which were largely sustained over 10 min, Fig. 3A). At PE concentrations of 300 nM, the average AUC was 101.1 ± 25.9 mN.s and at 1 μM PE, this was increased to 255.1 ± 58.5 mN.s (Fig. 3A, $n = 6$). Across 6 experiments, the EC_{50} value for PE on male USM contractions was 1.3 μM ($n = 6$). To verify that such responses were reproducible, we repeated the PE applications on the same tissues after 4 × 15 min washes, and when contractions of both response curves were compared, there was no statistical differences in the areas of contraction ($P > 0.7$) or in EC_{50} values ($P = 0.6$, $n = 6$, data not shown).

We next tested effects of the potent and selective ANO1 inhibitor Ani9 [29] on PE-induced contractions of male USM. As shown in Fig. 3A&B, in the same tissues, after washout of the first series of PE concentrations, reintroduction of cumulative PE doses after 30-minute incubation with Ani9 (3 μM) failed to impact either the EC_{50} (1.3 μM, $P = 0.6$) or AUC ($P = 0.5$) of PE responses at any concentration tested ($n = 6$, Fig. 3D). In addition, Ani9 had no effect on the resting level of tone of USM (Fig. 3C&E, $n = 6$, $P = 0.9$).

We further investigated Ani9 effects on neurally-evoked responses of USM. We contracted USM using electrical field stimulation (EFS) at a range of stimulation frequencies (1, 2, 5, 10 and 20 Hz, see Methods) to induce contractions that increased in amplitude with increased EFS frequency, these responses were abolished by tetrodotoxin indicating they were neurogenic (Fig. 4A&B). EFS-evoked contractions were reproducible after a time interval of 30 min ($n = 6$, data not shown) and were abolished by 1 μM tetrodotoxin (TTX) at all EFS frequencies (Fig. 4A&C, $n = 6$). When tissues were pre-incubated with Ani9 (3 μM) for 30-mins (Fig. 4B) EFS-induced contractions were unaffected at all frequencies (Fig. 4B&D, $P > 0.19$, $n = 6$).

Effects of ANO1 Inhibition on USM Ca^{2+} signals

The underlying cellular behaviour that leads to urethral tone in mice is the firing of intracellular Ca^{2+} release events in USMC[36,41], which are increased in frequency by PE[36] or EFS[25]. In a further series of experiments, we tested the effects of Ani9 on these basal USMC Ca^{2+} events. USMC recorded from Acta2-GCaMP8.1 mice in situ were spontaneously active and exhibited asynchronous Ca^{2+} activity throughout the muscle bundle, as previously described in male USM tissues imaged with GCaMP3[36]. Ani9 failed to cause any significant changes in Ca^{2+} activity of either male ($n = 5$, c = 10, Fig. 5A&B) or female urethra ($n = 6$, c = 15, Fig. 5C&D). It did not affect the frequency ($P = 0.7$), amplitude ($P = 0.9$), duration ($P = 0.7$), or spread ($P = 0.7$) of male USMC Ca^{2+} events ($n = 5$, c = 10), as shown in Fig. 5B. Similarly, in female urethra there was no significant change in frequency ($P = 0.16$), amplitude ($P = 0.9$), duration ($P = 0.13$) or spread ($P = 0.9$, $n = 6$, c = 15, Fig. 5D).

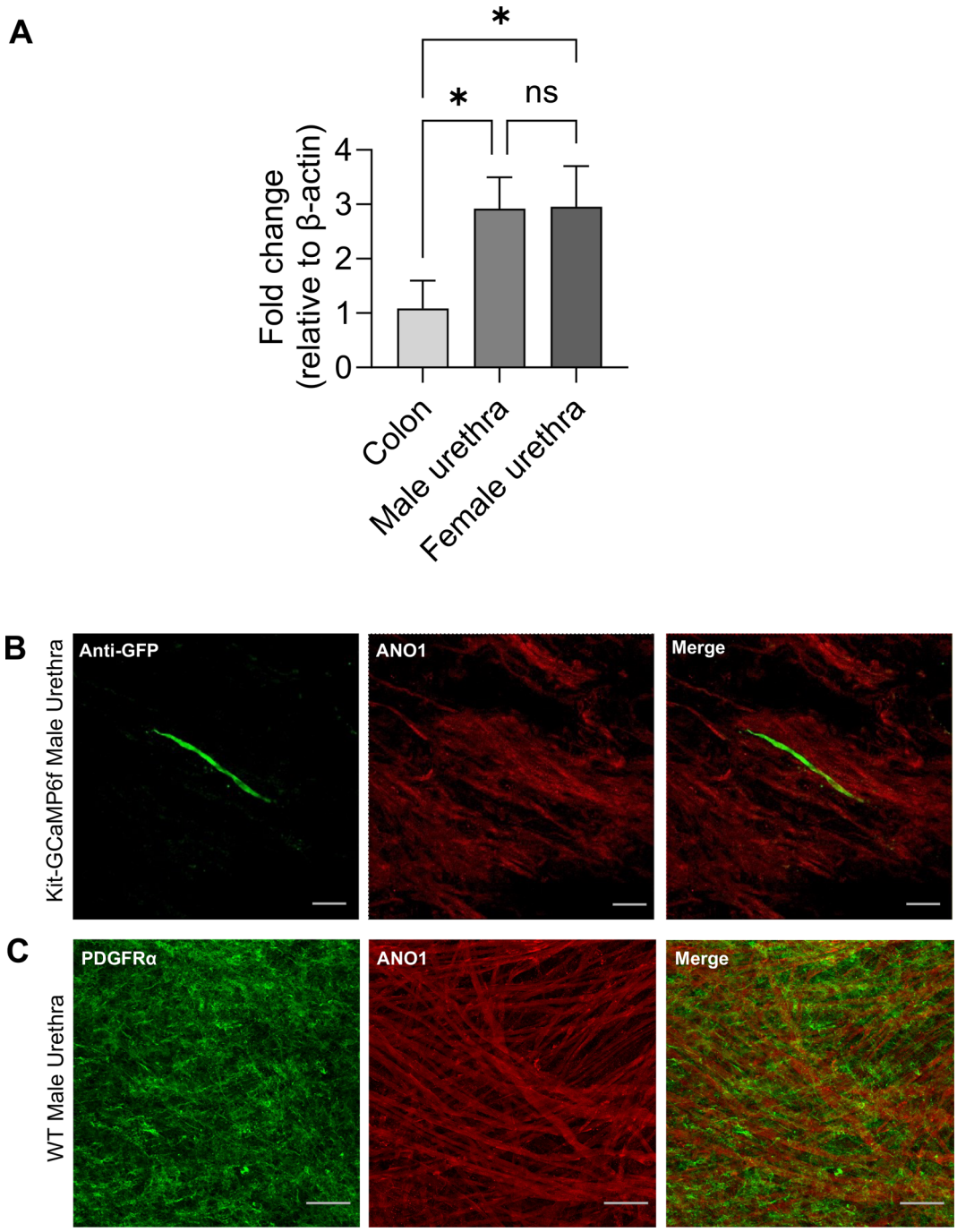

Fig. 1. Expression of Ano1 transcript in urethral tissues and ANO1 protein in mouse urethral interstitial cells. (**A**) Real-time PCR analyses showing the gene expression of *Ano1* normalized to β-actin gene expression (endogenous control) in male, female urethra and proximal colon. Fold change was calculated by taking proximal colon as a calibration control ($2^{-\Delta\Delta CT}$). Data represents the comparison of *Ano1* fold change expression relative to β-actin in male ($n=3$), female urethra ($n=3$) and proximal colon ($n=3$). (**B**) Representative images of double immuno-labelling for anti-GFP (ICC-LC, green) and ANO1 (red) in Kit-GCaMP6f mouse urethra ($n=5$) captured at 40x magnification. (**C**) Representative images of PDGFRα^{+} cells (green) and ANO1 (red) in WT male mouse urethra ($n=3$) captured at 20x magnification. Scale bar: 50 µm in all panels.

Ani9 inhibits ANO1 currents recorded from HEK 293 cells

The data shown in Fig. 6 demonstrates that Ani9 was an effective inhibitor of ANO1 currents. We examined the effects of Ani9 (100 nM) on human ANO1 currents recorded from HEK 293 cells using the whole cell configuration of the patch clamp technique. Currents were evoked by voltage steps from −100 mV to +120 mV in 20 mV increments, each lasting 1 s, from a holding potential of -60 mV. Following the test potentials, a

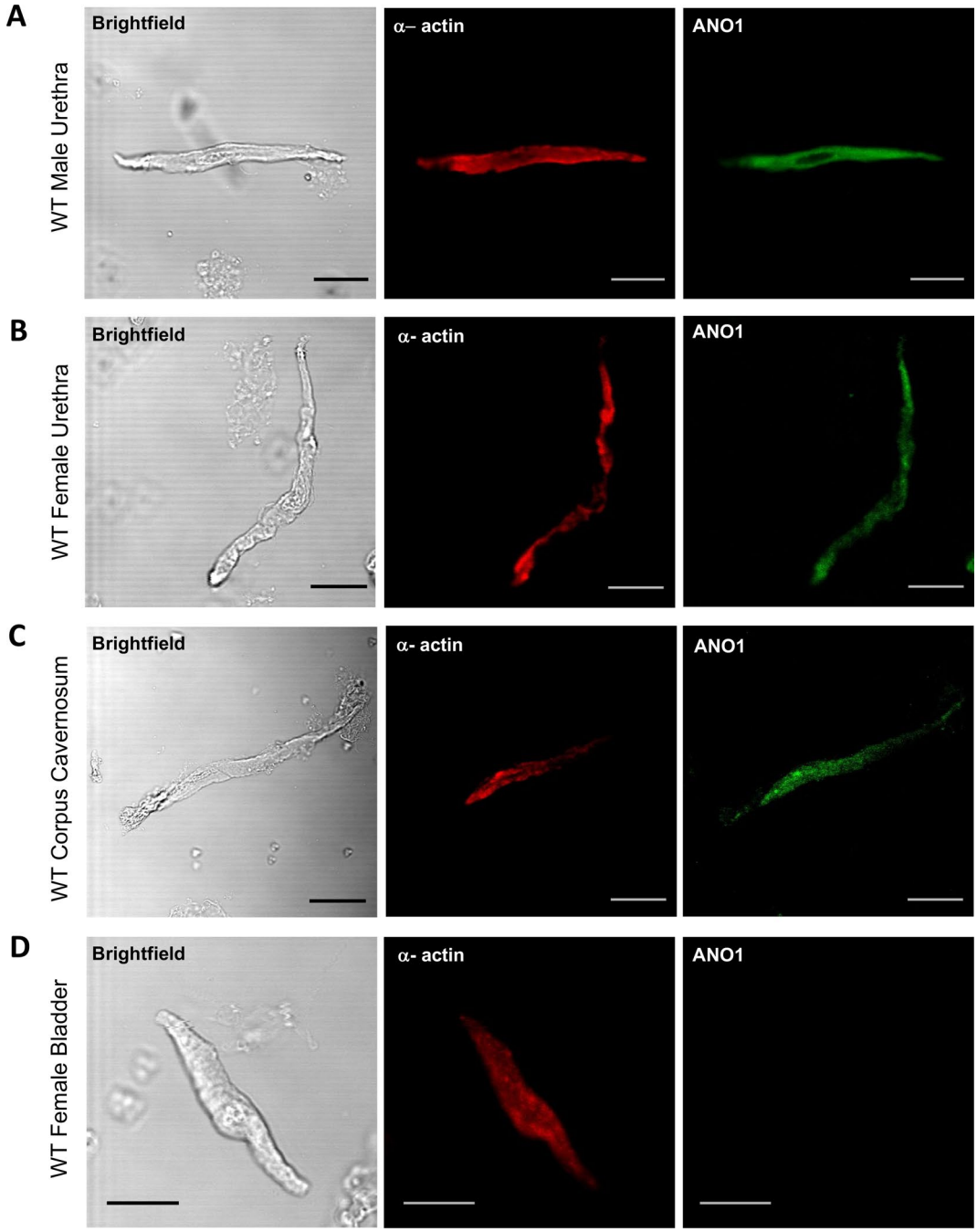

Fig. 2. ANO1 is expressed in urethral smooth muscle cells. (**A**) Representative images of urethral SMC (USMC) captured in brightfield and at different wavelengths (488 nm and 555 nm) to show double immuno-labelling for α-actin (red) and ANO1 (green) from WT male urethra ($n = 3$) and (**B**) female urethra ($n = 3$). (**C**) Representative images of corpus cavernosum SMC captured in brightfield and at different wavelengths (488 nm and 555 nm) to show double immuno-labelling for α-actin (red) and ANO1 (green) ($n = 3$) (**D**) Representative images of bladder SMC captured in brightfield and at different wavelengths (488 nm and 555 nm) to show immuno-labelling for α-actin (red) and a lack of ANO1 labelling in the same cell (green) ($n = 3$). Scale bar: 20 μm in all panels.

step to -80 mV for 500 milliseconds was applied to generate tail currents. The amplitude of the outward current was maximum at the end of the sweep and this was measured to generate current-voltage relationships (I-V). Representative ANO1 currents recorded prior to and during the application of Ani9 (100 nM) are illustrated in Fig. 6A&B, respectively. These recordings demonstrated that Ani9 significantly inhibited ANO1 currents across the voltage range. Summary I-V plots, in the absence and presence of Ani9, are shown in Fig. 6C. There was a significant reduction in current amplitude across the voltage range in presence of Ani9 (Fig. 6C, $n = 13$). At a test

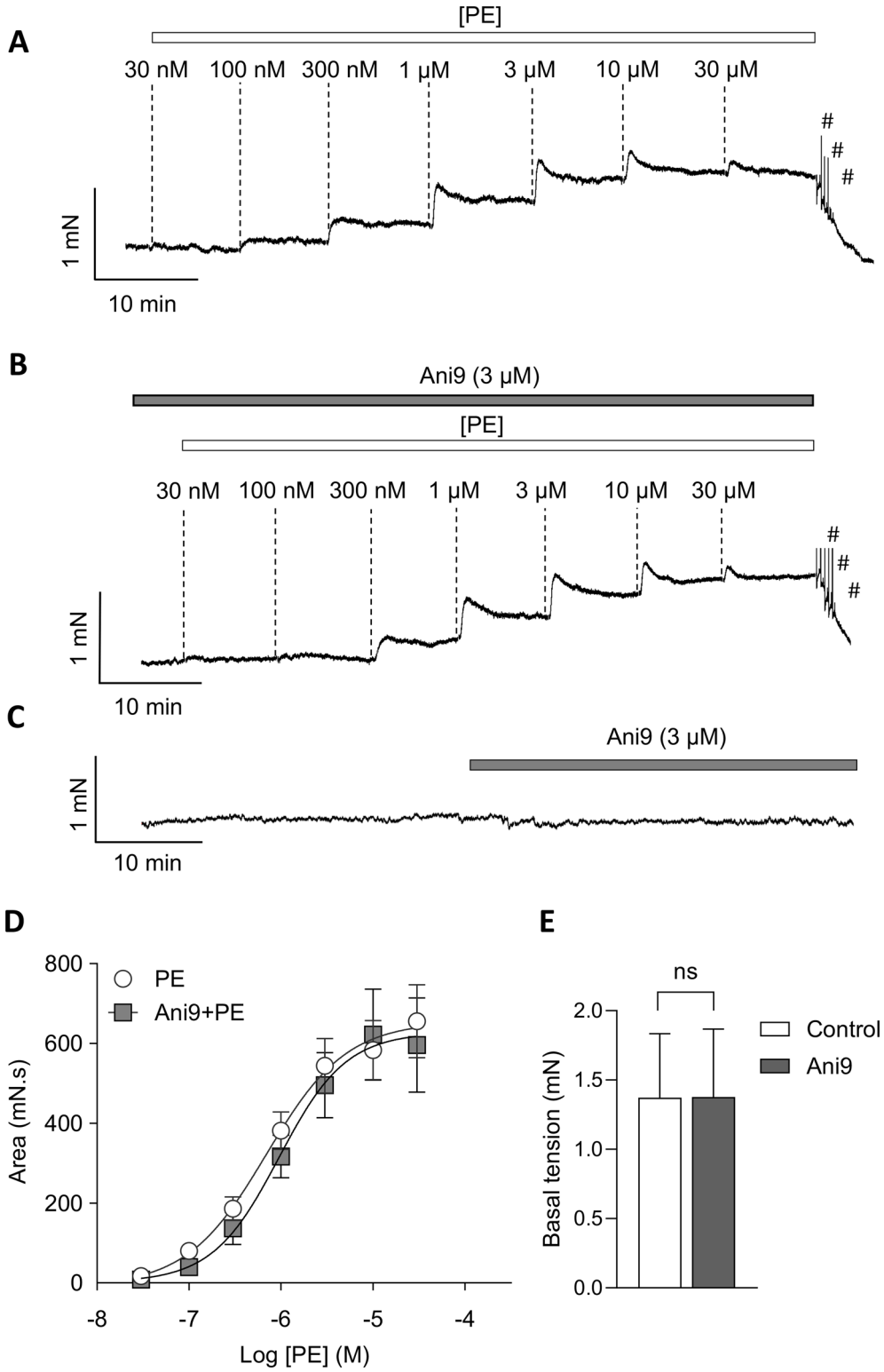

Fig. 3. The specific and potent ANO1 inhibitor Ani9 does not affect urethral contractions evoked by phenylephrine (PE) or basal tone. (**A**) Representative isometric tension trace showing male USM contractions induced by increasing phenylephrine (PE) concentrations (30 nM – 30 µM), (# represents washing). (**B**) In the same tissues shown in panel A, after 30 min incubation with Ani9 (3 µM), the cumulative PE doses were reapplied. (# represents washing). (**C**) Representative contractile trace of Ani9 (3 µM) on basal male urethral tone. (**D**) Summary effects of Ani9 on PE dose responses curves in male USMC ($n = 6$). (**E**) Summary effects of Ani9 on basal resting tone in males USMC ($n = 6$).

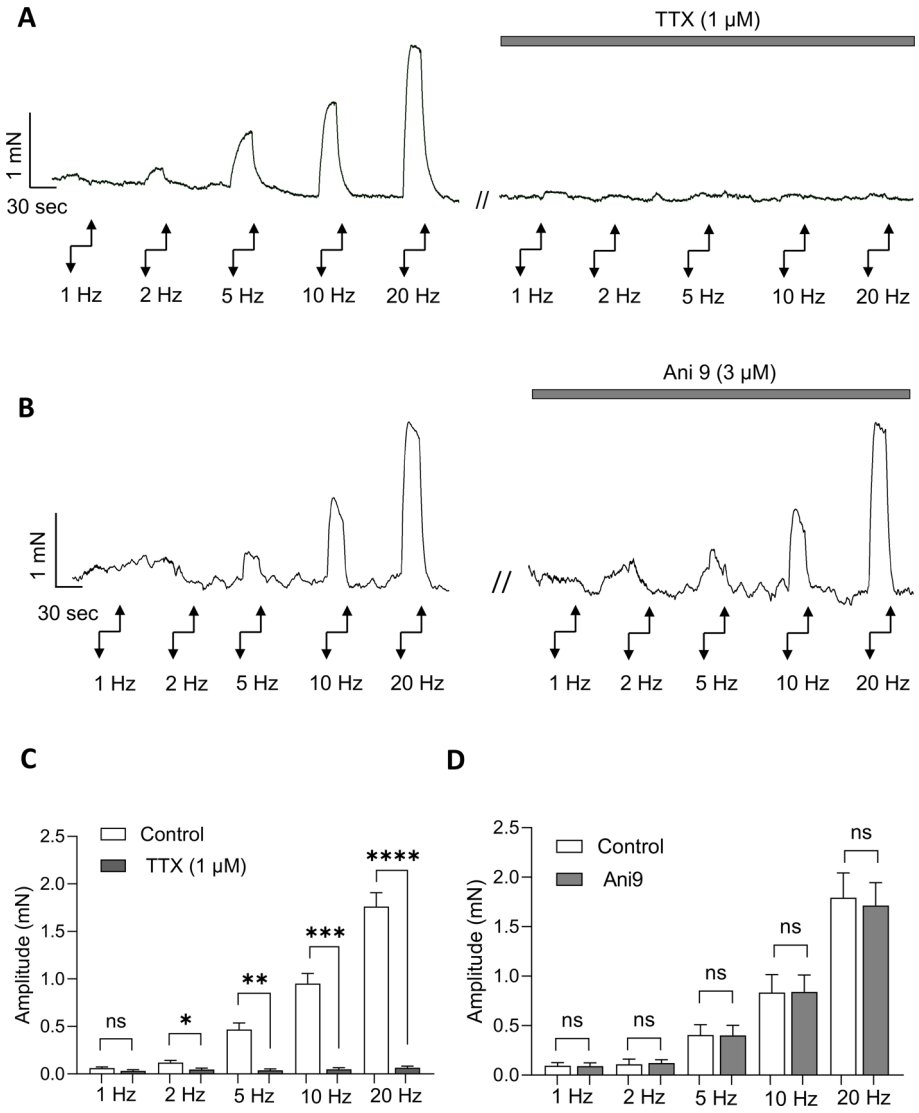

Fig. 4. Ani9 does not affect electrical field stimulation (EFS)-evoked contractions of male murine USM. (**A**) EFS evokes contractions of male USM, which are increased in amplitude as EFS frequency is increased. These responses were abolished by tetrodotoxin (TTX, 1μM). (**B**) EFS evoked-contractions of male USM responses were unaffected by Ani9 (3μM). (**C**) Summary effects of TTX on EFS induced contraction amplitude in USM ($n=6$). (**D**) Summary effects of Ani9 on EFS induced contraction amplitude in USM ($n=6$).

potential of +120 mV, mean current amplitude decreased from 2.8 ± 0.4 nA to 0.3 ± 0.1 nA in Ani9 ($P<0.0001$, $n=13$, Fig. 6C). These data indicated that Ani9 is a potent inhibitor of ANO1 channel activity.

To check the efficacy of Ani9 on tissue responses, we performed isometric tension recordings of spontaneous phasic contractions of mouse proximal colon, as it is well established that ANO1 channels expressed in colonic ICC play a major role in motility[42]. We found that Ani9 (3 μM) had an immediate inhibitory effect on colonic contractions (Fig. 7A, $n=6$) by reducing average amplitude from 11.6 ± 2.9 to 4.6 ± 1.3 mN ($P=0.02$, Fig. 7B, $n=6$), and the frequency from 3.4 ± 0.7 to 1.7 ± 0.4 min^{-1} ($P=0.004$, Fig. 7C, $n=6$). These experiments suggested that in our hands, in other visceral USM tissues, Ani9 was effective in inhibiting contractions in organ bath experiments. We also studied effects of Ani9 on Ca^{2+} signals generated in proximal colon SMC from Acta2-GCaMP8.1 mice. In these recordings (40x objective), strips of circular orientated proximal colon SMC generated regular propagating waves, or flashes, of Ca^{2+} that lasted for up to 5 s each, and propagated rapidly across the tissue ~ 5 times per minute. These colonic Ca^{2+} signals induced massive contractions of colonic muscles, making analysis of individual cells impossible. Instead, Ca^{2+} signals across the entire field of view in a 30 s recording were plotted against time to generate plots of Ca^{2+} activity from which the amplitude, frequency and duration of Ca^{2+} waves across the whole FOV could be quantified. Plots of this activity in Fig. 7D (summated Ca^{2+} signal from the entire 30 s recording) shows reduced Ca^{2+} activity in the presence of Ani9 compared to control (Fig. 7D). Ani9 significantly reduced the Ca^{2+} events of proximal colon ($n=7$, Fig. 7D&E) by reducing frequency from 5.4 ± 0.8 to 2.8 ± 0.7 min^{-1} ($P=0.015$), amplitude from 1 ± 0.3 to 0.4 ± 0.1 $\Delta F/F_0$ ($P=0.04$) and duration from 4.9 ± 1.1 to 2.9 ± 0.75 s ($P=0.03$).

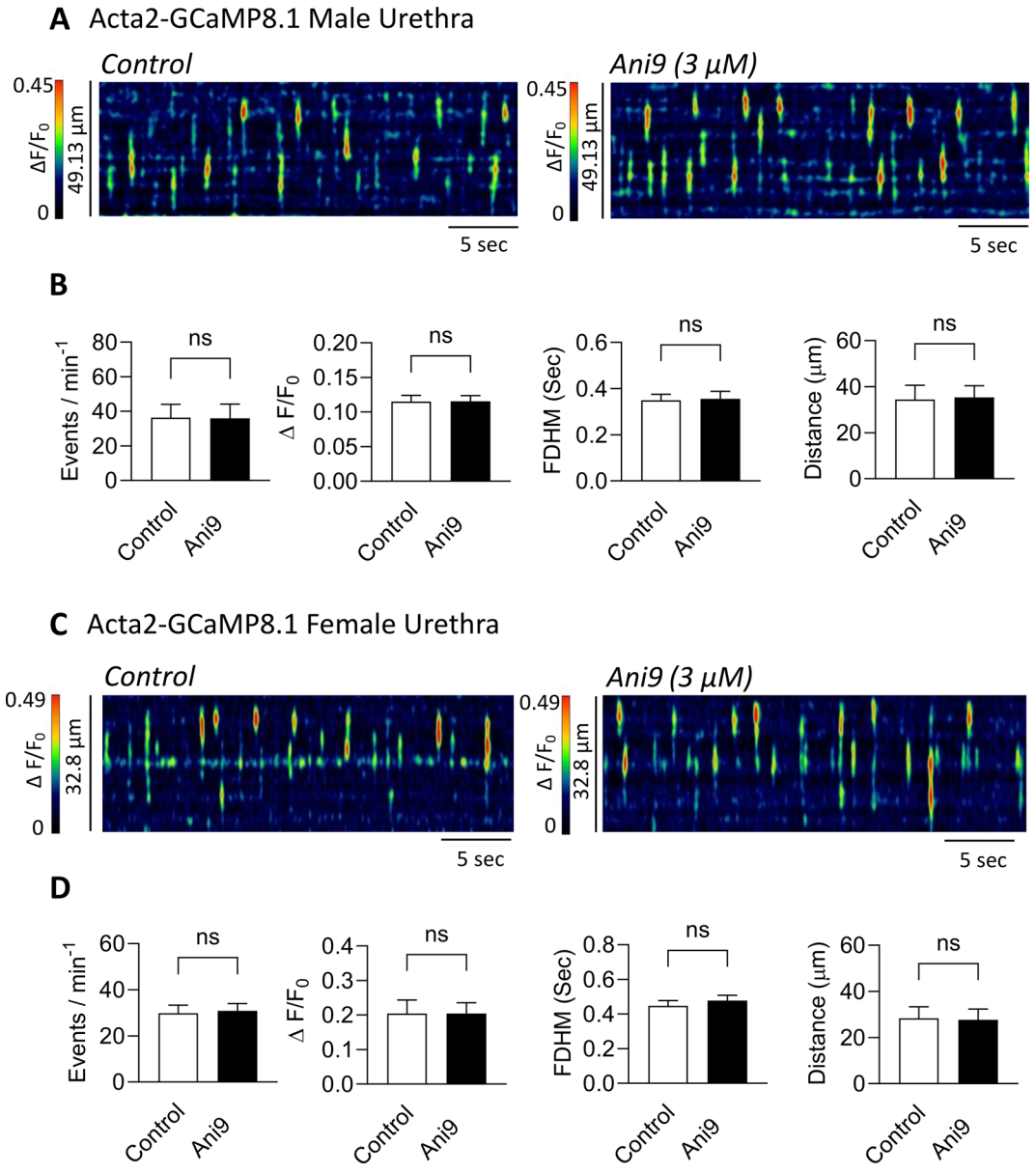

Fig. 5. Spontaneous USMC Ca^{2+} events do not depend on ANO1 channels. (**A**) Spatiotemporal maps (STMs) of Ca^{2+} events in male USMC recorded in situ from an Acta2-GCaMP8.1 mouse during control conditions and after incubation with 3 µM Ani9. (**B**) Summary effects of Ani9 on male USMC Ca^{2+} event frequency, amplitude, duration and spatial spread ($n = 5$, c = 10). (**C**) STMs of Ca^{2+} events in female USMC recorded in situ from an Acta2-GCaMP8.1 mouse during control conditions and after incubation with 3 µM Ani9. (**D**) Summary effects of Ani9 on female USMC Ca^{2+} event frequency, amplitude, duration and spatial spread ($n = 6$, c = 15).

To demonstrate that USM contractions evoked by either PE or EFS could be reduced by appropriate means, we tested effects of 2-APB (2-Aminoethoxydiphenyl borate). 2-APB is an IP_3R antagonist, which should reduce contractions of USM induced by exogenous application of PE or release of noradrenaline following stimulation of intramural nerves. We found that 2-APB (100 µM) effectively reduced PE-evoked contractions at all concentrations tested ($n = 6$, Fig. 8A, B&D). For example, at 300 nM PE, contractile AUC was reduced from 335.8 ± 92.2 mN.s to 4.68 ± 4.1 mN.s ($P = 0.0005$, Fig. 8D, $n = 6$) and at 30 µM PE, AUC of evoked responses were reduced from 1128.3 ± 173.4 mN.s to 83.7 ± 58.1 mN.s ($P < 0.0001$, Fig. 8D, $n = 6$). Similarly, 2-APB abolished EFS-evoked contractions at all stimulation frequencies ($n = 6$, Fig. 8C&E). These controls established that our observed agonist and EFS responses could be inhibited by pharmacological agents.

We further tested other Ca^{2+}-activated-Cl^- channel antagonists that may target other channels than ANO1 on EFS-evoked responses. The non-selective Ca^{2+}-activated-Cl^- channel antagonist, niflumic acid (100 µM) significantly reduced EFS responses at all frequencies of stimulation above 2 Hz (Fig. 9A&C, $n = 5$), for example reducing EFS-evoked contraction amplitude at 5 Hz by 70% ($P = 0.0003$) and 42% at 20 Hz ($P < 0.0001$).

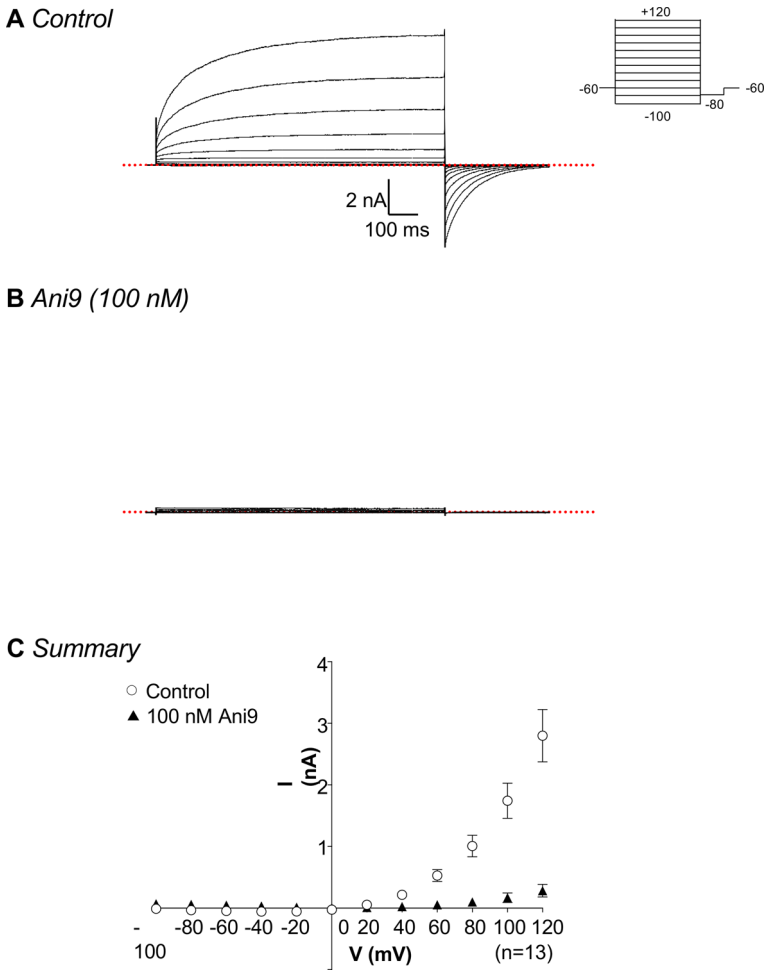

Fig. 6. Effect of 100 nM Ani9 on ANO1 currents in HEK 293 cells. (**A**) Typical family of whole cell currents obtained from human ANO1 channels expressed in HEK cells with 100 nM intracellular Ca^{2+}. The voltage clamp protocol is described in the inset. Dotted lines represent the zero current level. (**B**) Effect of 100 nM Ani9 on currents from the same cell. (**C**) Summary of current voltage (I-V) relationship obtained by measuring outward currents at the end of the sweep in thirteen cells before (open circle) and during (closed triangle) application of Ani9 ($n = 13$).

$CaCC_{inh}$A01 (10 μM), a second generation ANO1 antagonist, failed to significantly affect EFS-evoked contractions of USM at any stimulation frequency, similar to Ani9 (Fig. 9B&D, $n = 5$). However, in the continued presence of $CaCC_{inh}$A01, niflumic acid was effective in reducing EFS responses in a similar manner to when $CaCC_{inh}$A01 was absent (Fig. 9B&D, $n = 5$).

The preceding experiments using PE and EFS were all conducted on male tissue, as female mouse USM contracts weakly in response to excitatory EFS or to PE[37,43]. As an alternative means of evoking contractions of female USM, we pre-contracted female tissues with arginine vasopressin (AVP, antidiuretic hormone), a vasopressin 1_A receptor ($V1_AR$) agonist. AVP activates G_q - phospholipase C - IP_3 signalling pathways, similar to adrenergic stimulation, thereby triggering IP_3R and SR Ca^{2+} release[44]. We initially attempted to perform concentration response curves with AVP in a similar manner to our previous experiments with PE on male tissues, however we found that in contrast to PE-evoked contractions, responses elicited by AVP in females were not reproducible, as it was not possible to fully wash out AVP and replicate concentration response curves in the same tissue (data not shown). Instead, we applied a single concentration of AVP to female tissues (10 nM), which immediately led to a sustained contraction (Fig. 10A&B). When Ani9 (3 μM) was applied to female USM precontracted with AVP in this manner, there was no effect (Fig. 10A&C, $P = 0.09$ A $n = 6$), whereas subsequent addition of 2-APB (100 μM) abolished AVP-induced contraction in females (Fig. 10A&C, $P = 0.0005$, $n = 6$). $CaCC_{inh}$A01 (10 μM) caused a slight reduction in the AVP-evoked contractions of female tissues (14%, Fig. 10B) but this was not statistically significant (Fig. 10D, $P = 0.4$, $n = 6$). Further addition of niflumic acid almost abolished the AVP responses (Fig. 10D, $n = 6$).

Discussion

In this study, we used qPCR and immunohisto / cyto-chemistry to study cellular expression of ANO1 channels in mouse USM. We found that ANO1 channels were expressed in murine USMC and not in specialized

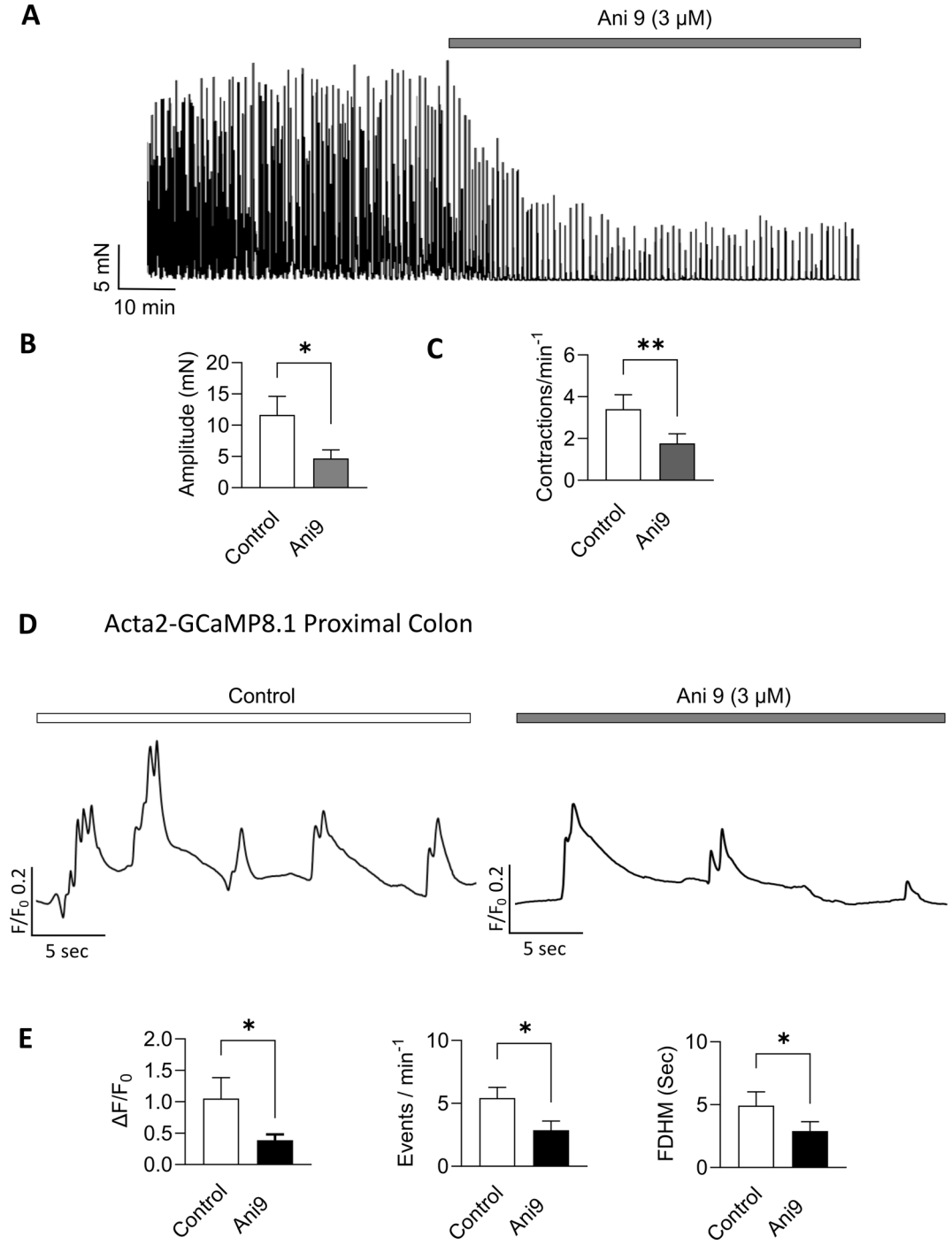

Fig. 7. Ani9 inhibits phasic contractions and basal Ca^{2+} activity of mouse proximal colon. (**A**) Isometric tension recording of phasic contractions from male mouse proximal colon in the absence and presence of Ani9 (3 μM). (**B**) Summary effects of Ani9 on the amplitude of phasic contractions in mouse proximal colon. (**C**) Summary effects of Ani9 on the amplitude and frequency of phasic contractions in mouse proximal colon (**D**) Plot profile of spontaneous Ca^{2+} signals recorded from an entire field of view (40x objective) of proximal colon from an Acta2-GCaMP8.1 mouse in the absence (control) and presence of 3 μM Ani9. . (**E**) Summary of 3 μM Ani9 effects on amplitude, frequency and duration of Ca^{2+} events in proximal colon ($n = 6$).

interstitial cells. Despite cellular expression of ANO1, a specific and potent antagonist of ANO1 channels, Ani9, at concentrations that significantly reduced colonic contractions and Ca^{2+} signals, failed to impact male or female urethral contractions or spontaneous Ca^{2+} signals.

Cellular expression and function of ANO1 channels in USMC appears to be species dependent. Previous studies suggested ANO1 expressed in a specialized interstitial cell may exert an excitatory influence on USMC,

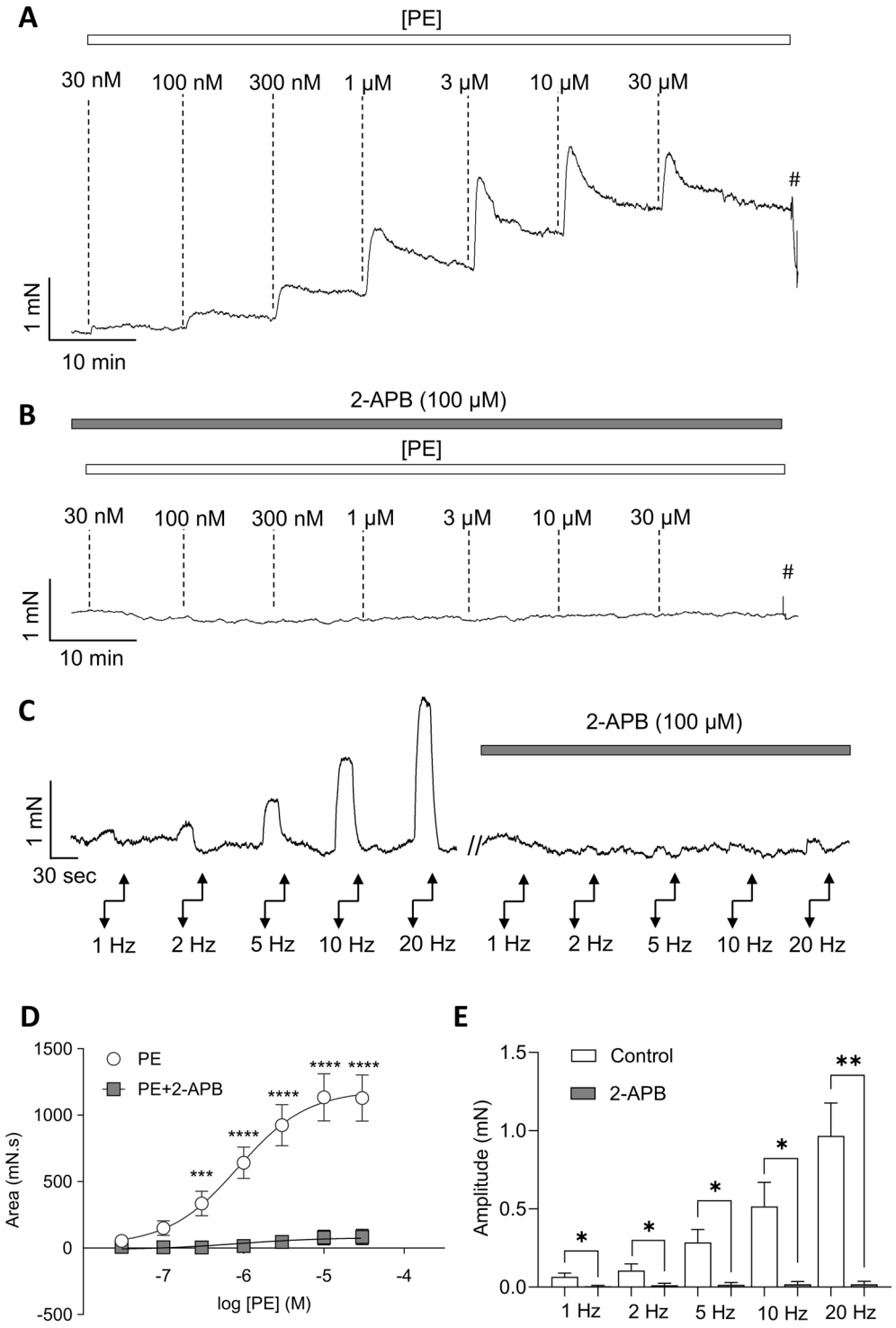

Fig. 8. IP_3 receptor antagonist 2-APB abolished agonist and EFS-evoked contractions in male USM. (**A**) Representative isometric tension recording from male USM showing contractions induced by increasing PE concentrations (30 nM – 30 µM) were abolished by the IP_3-receptor (IP_3R) antagonist, 2-APB (100 µM) (**B**). (**C**) Representative isometric tension recording from male USM showing contractions induced by EFS were inhibited by the IP_3R antagonist, 2-APB (100 µM). (**D**) Summary effects of 2-APB on PE evoked contractions of male USM ($n = 6$). (**E**) Summary effects of 2-APB on EFS evoked contraction amplitude of male USM ($n = 6$).

serving as a type of pacemaker conductance to modulate USMC excitability[7,45] similar to ANO1 found in ICC of the gastrointestinal tract[6,46,47]. In rabbit, transcriptional *Ano1* expression is largely restricted to specialized interstitial cells, referred to here as ICC-LC[8], which exhibit robust Ca^{2+}-activated Cl^- current and spontaneous activity lacking in rabbit USMC[8,20]. However, studies from sheep and rodents show ICC-LC lack ANO1 at the

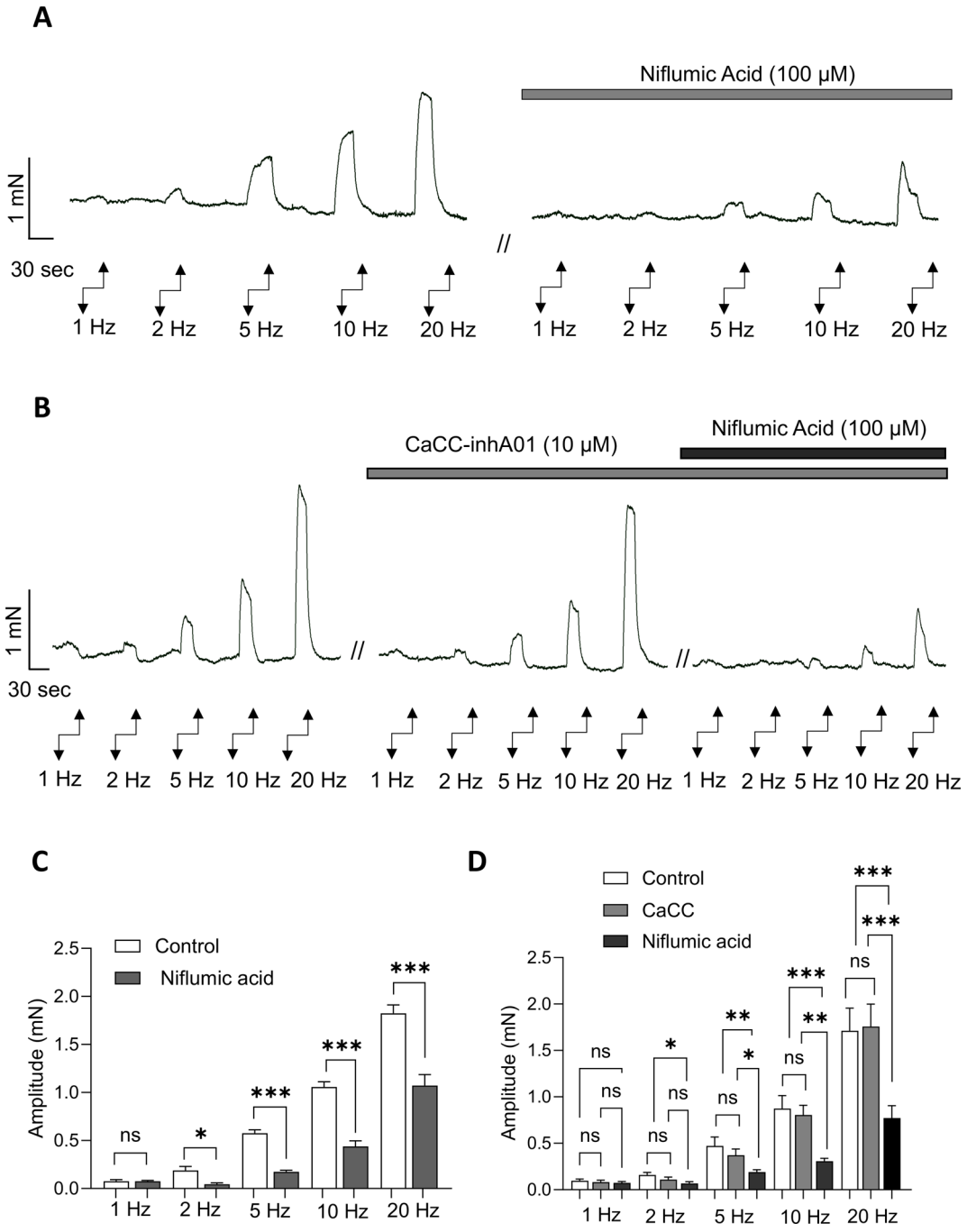

Fig. 9. EFS-evoked contractions of male USM are inhibited by niflumic acid but not $CaCC_{inh}A01$. (**A**) Representative isometric tension recording from male USM showing contractions induced by EFS were inhibited by the non-selective Ca^{2+}-activated-Cl^- channel antagonist, niflumic acid (100 μM). (**B**) Representative isometric tension recording from male USM showing contractions induced by EFS were unaffected by $CaCC_{inh}A01$ but were subsequently reduced by the non-selective Ca^{2+}-activated-Cl^- channel antagonist, niflumic acid (100 μM). (**C**) Summary effects of niflumic acid on EFS evoked contraction amplitude of male USM ($n = 5$). (**D**) Summary effects of $CaCC_{inh}A01$ and niflumic acid on EFS evoked contraction amplitude of male USM ($n = 5$).

protein level, and ANO1 is expressed in USMC[9]. In our experiments, we sought to clarify this by identifying ICC-LC in mouse tissues in situ, by labelling KitGCaMP urethral tissues with antibodies against GFP as described previously[25]. With this approach, we determined that murine ICC-LC, which unlike USMC had a characteristic elongated morphology and were not arranged in bundles, did not co-label with antibodies against ANO1. In other urinary tract and reproductive tissues, ANO1 expression is found in specialized PDGFRα$^+$ cells[39,40].

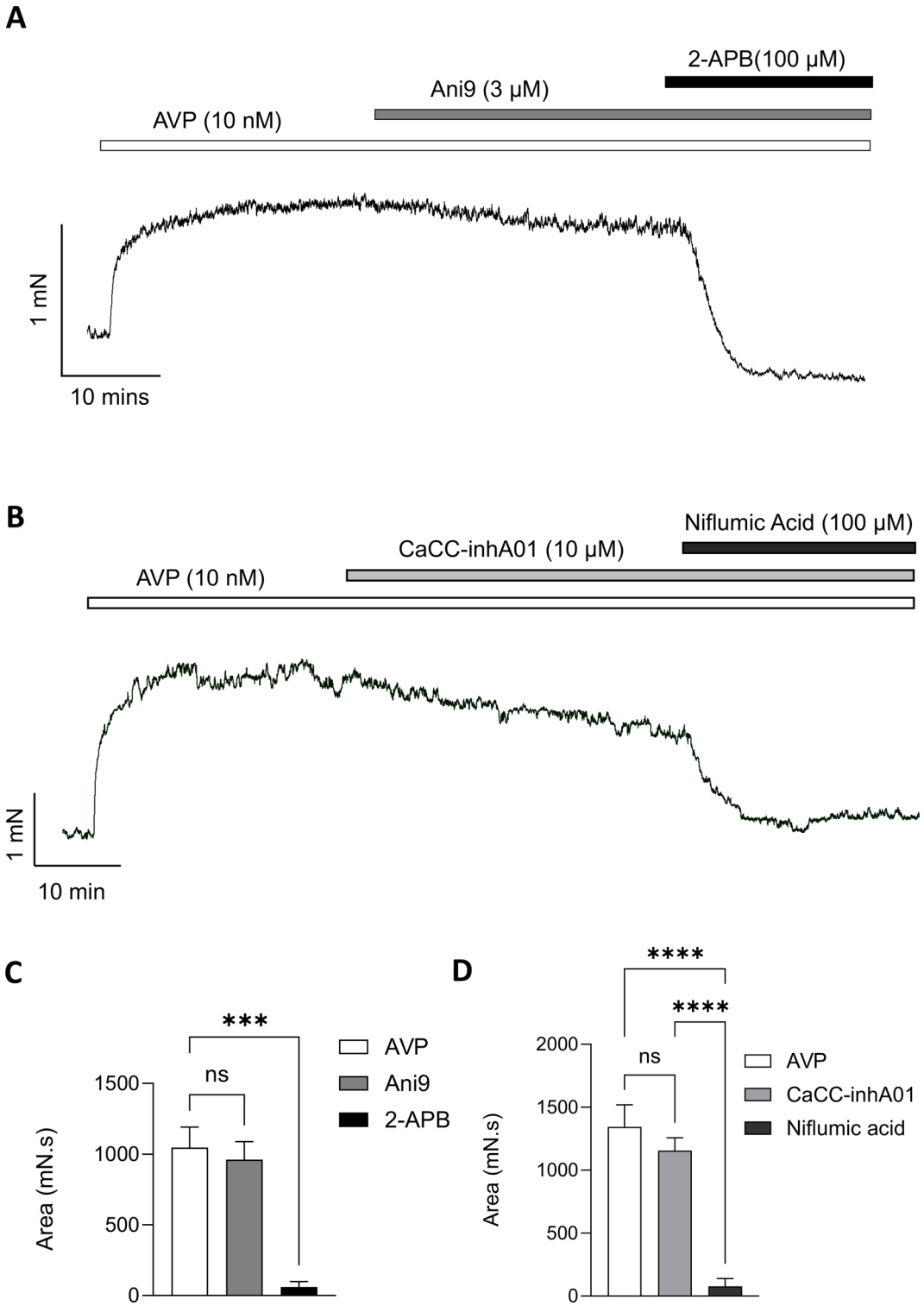

Fig. 10. Ani9 does not affect AVP induced contraction in female USM. (**A**) Representative data showing effects of Ani9 (3 μM) and 2-APB (100 μM) on AVP (10 nM) induced contractions of female USM. (**B**) Representative data showing effects of $CaCC_{inh}A01$ (10 μM) and niflumic acid (100 μM) on AVP (10 nM) induced contractions of female USM. (**C**) Summary effects of Ani9 and 2-APB on AVP evoked contractions of female USM ($n = 6$). (**D**) Summary effects of $CaCC\text{-}_{inh}A01$ and niflumic acid on AVP evoked contractions of female USM ($n = 6$).

However, we found that ANO1 antibodies did not co-label with PDGFRα, suggesting that ANO1 expression was lacking in interstitial cells in mouse, but abundantly expressed in USMC.

Our qPCR data showed that transcripts for ANO1 channels were expressed at relatively similar levels in male and female USM, and immunolabelling of isolated male and female USMC showed similar patterns of ANO1 expression. This is in contrast to another study which postulated that differences in ANO1 expression accounted for sex differences in tone in both mice and human USM tissues[48]. In this previous study, it was claimed that female USMC expressed twice as much ANO1 protein as determined by western blotting. The reasons for these differences in observations is currently not clear but may reflect differences in ANO1 antibody selection between different experimental groups.

Differential ANO1 expression, or down regulation of ANO1 in mouse USMC has been proposed to account for sex differences in levels of urethral tone[48] and loss of USM contractility in hypertriglyceridemia[49]. Evidence for these hypotheses includes inhibition of USM tone by the pharmacological agent T16inh-A01[50], stimulation of tone by the ANO1 activator EACT[48], and a reported loss of USM tone in animals lacking ANO1 in USMC[50]. However, most of the evidence for a functional role of ANO1 in USM contractility derives from pharmacological inhibitors such as DIDS, MONNA, $CaCC_{inh}A01$ or $T16_{inh}A01$. These drugs are now known to have numerous pronounced off target effects on L-type Ca^{2+} channels and SR Ca^{2+} release mechanisms[26–28], which could affect interpretation of these data.

In our experiments, we used a potent and selective ANO1 channel inhibitor, Ani9[29], which does not demonstrate these off target effects in smooth muscle[27,28,30]. In our hands, Ani9, as well another ANO1 channel inhibitor, $CaCC_{inh}A01$, failed to significantly impact USM contractions evoked by agonists such as PE or AVP in male and female tissues, nor EFS-evoked contractions of male USM. In addition, Ani9 did not impact the basal underlying Ca^{2+} waves in USMC that generate tone. Importantly, we verified the efficacy of Ani9 in our experiments, by demonstrating that Ani9 significantly inhibited human ANO1 currents in HEK 293 cells at concentrations 30 times less than those tested on urethral tissues. In addition, the same concentration of Ani9 tested on USM significantly reduced spontaneous phasic contractions and Ca^{2+} flashes of mouse proximal colon.

While Ani9 and $CaCC_{inh}A01$ had no significant effects on urethral contractions, we found potent effects of niflumic acid, a non-selective Ca^{2+}-activated-Cl^- channel inhibitor, on EFS and AVP-evoked contractions of both male and female USM. This leaves open the possibility that Ca^{2+}-activated-Cl^- channels other than ANO1 may be important in regulating agonist and neurally mediated contractions of USM. However, these data must be interpretated cautiously, as niflumic acid is known to exert numerous off target effects which may account for our findings, such as leaking Ca^{2+} from the SR[27,51], blockade of voltage-dependent Ca^{2+} channels[52], modulating ryanodine receptors[53] and opening K^+ channels[54]. Similarly, in our experiments on AVP responses in female USM, we observed a slight but non-statistically significant reduction in AVP-evoked contractions in the presence of $CaCC_{inh}A01$. However, this agent is also known to exhibit off-target effects (which Ani9 does not under the same conditions) such as low levels of SR Ca^{2+} release in SMC[28] and possible inhibitory effects on IP_3Rs[27], which might account for these slight reductions in AVP responses.

Similar to our findings in mouse, Ani9 also did not reduce USM tone or contractions elicited by EFS in porcine USM, all of which were significantly reduced by nifedipine[55]. This suggests that even when a clear need for voltage-dependent L-type Ca^{2+} channels is apparent for myogenic tone or evoked contractions in USM, ANO1 channels do not provide a depolarizing influence to this mechanism in certain species. While our findings certainly do not rule out a functional role for ANO1 in rabbit USM, (where abundant ANO1 current is found in ICC-LC) or human USM (where ANO1 expression remains to be clearly determined), future experiments using ANO1 channel inhibitors such as Ani9 on rabbit and human USM would help clarify this question.

We emphasise that our findings do not preclude a role of ANO1 channels in modulating USMC outside of the parameters of our experiments. We tested the effects of ANO1 inhibition on basal Ca^{2+} signalling, agonist and EFS-evoked contractions of USMC using standard experimental protocols. It is possible that effects of ANO1 channel inhibitors would only manifest under other experimental conditions. For example, in airway smooth muscle (ASM), knockout of ANO1 has little effect on cholinergic-induced contractions[56], and Ani9 has neglible effects on cholinergic mediated contractions[57]. However, cholinergic stimulation of ASM involves both activation of postjunctional muscarinic type 2 and 3 receptors (M2/3Rs), with M2R activation enhancing the effects of M3Rs[58]. In a 2025 study, using protocols to isolate the M2R-mediated potentiation of cholinergic stimulation on murine ASM, Ani9 reduced resultant contractions by 50%[57]. These data reveal that the ability to observe contributions of ANO1 channels to smooth muscle activity can be protocol dependent. Whether ANO1 inhibition may affect USMC using variations of our current protocols is unknown, and warrants further investigation. It could also be true that ANO1 could be contribute to other physiological mechanisms in the urethra other than modulating USMC contractility. In arterial SMC, ANO1 expression is inversely linked to vascular remodelling in the brain[59]. Whether ANO1 expressed in USM might contribute to tissue remodelling or proliferation is currently unknown but also warrants further investigation.

In conclusion, we have established that the Ca^{2+}-activated Cl^- channel ANO1 is expressed in both male and female mouse USM tissues, with no obvious sex differences in transcriptional or protein expression. At the cellular level, ANO1 expression is confined to USMC rather than specialized populations of ICC-LC or $PDGFR\alpha^+$ cells. Despite expression of ANO1 in USMC, these channels do not appear to functionally contribute to basal Ca^{2+} signalling, or agonist and neurally evoked contractions in murine USM. However, this does not rule out that ANO1 may regulate USMC activity under specific circumstances not yet elucidated in the urethra.

Data availability

The datasets presented in this study are available from the corresponding authour upon reasonable request.

Received: 20 January 2025; Accepted: 2 May 2025

Published online: 19 May 2025

References

1. Huang, F. et al. Studies on expression and function of the TMEM16A calcium-activated chloride channel. *Proc. Natl. Acad. Sci. U S A*. **106**, 21413–21418. https://doi.org/10.1073/pnas.0911935106 (2009).
2. Bulley, S. & Jaggar, J. H. Cl^- channels in smooth muscle cells. *Pflugers Arch.* **466**, 861–872. https://doi.org/10.1007/s00424-013-1357-2 (2014).
3. Aickin, C. C. & Brading, A. F. Measurement of intracellular chloride in guinea-pig Vas deferens by ion analysis, 36chloride efflux and micro-electrodes. *J. Physiol.* **326**, 139–154. https://doi.org/10.1113/jphysiol.1982.sp014182 (1982).
4. Leblanc, N. et al. Regulation of calcium-activated chloride channels in smooth muscle cells: a complex picture is emerging. *Can. J. Physiol. Pharmacol.* **83**, 541–556. https://doi.org/10.1139/y05-040 (2005).
5. Hawn, M. B., Akin, E., Hartzell, H. C., Greenwood, I. A. & Leblanc, N. Molecular mechanisms of activation and regulation of ANO1-Encoded Ca(2+)-Activated Cl(-) channels. *Channels (Austin)*. **15**, 569–603. https://doi.org/10.1080/19336950.2021.1975411 (2021).
6. Sanders, K. M., Zhu, M. H., Britton, F., Koh, S. D. & Ward, S. M. Anoctamins and Gastrointestinal smooth muscle excitability. *Exp. Physiol.* **97**, 200–206. https://doi.org/10.1113/expphysiol.2011.058248 (2012).
7. Drumm, B. T., Thornbury, K. D., Hollywood, M. A. & Sergeant, G. P. Role of Ano1 Ca(2+)-activated Cl(-) channels in generating urethral tone. *Am. J. Physiol. Ren. Physiol.* **320**, F525–f536. https://doi.org/10.1152/ajprenal.00520.2020 (2021).
8. Fedigan, S. et al. Effects of new-generation TMEM16A inhibitors on calcium-activated chloride currents in rabbit urethral interstitial cells of Cajal. *Pflugers Archiv Eur. J. Physiol.* **469**, 1443–1455. https://doi.org/10.1007/s00424-017-2028-5 (2017).
9. Sancho, M., Garcia-Pascual, A. & Triguero, D. Presence of the Ca2+-activated chloride channel Anoctamin 1 in the urethra and its role in excitatory neurotransmission. *AJP: Ren. Physiol.* **302**, F390–F400. https://doi.org/10.1152/ajprenal.00344.2011 (2012).
10. Brading, A. F. The physiology of the mammalian urinary outflow tract. *Exp. Physiol.* **84**, 215–221 (1999).
11. Greenland, J. E., Dass, N. & Brading, A. F. Intrinsic urethral closure mechanisms in the female pig. *Scandinavian J. Urol. Nephrol. Supplement*. **30**, 75–80 (1996).
12. Andersson, K. E. Neurotransmission and drug effects in urethral smooth muscle. *Scand. J. Urol. Nephrol. Suppl.* **35**, 26–34. https://doi.org/10.1080/003655901750174854 (2001).
13. de Groat, W. C. et al. Neural control of the urethra. *Scand J Urol Nephrol Suppl*, 35–43; discussion 106–125, (2001). https://doi.org/10.1080/003655901750174872
14. Waldeck, K., Ny, L., Persson, K. & Andersson, K. E. Mediators and mechanisms of relaxation in rabbit urethral smooth muscle. *Br. J. Pharmacol.* **123**, 617–624. https://doi.org/10.1038/sj.bjp.0701645 (1998).
15. Thornbury, K. D., Hollywood, M. A. & McHale, N. G. Mediation by nitric oxide of neurogenic relaxation of the urinary bladder neck muscle in sheep. *J. Physiol.* **451**, 133–144. https://doi.org/10.1113/jphysiol.1992.sp019157 (1992).
16. Hashitani, H., Van Helden, D. F. & Suzuki, H. Properties of spontaneous depolarizations in circular smooth muscle cells of rabbit urethra. *Br. J. Pharmacol.* **118**, 1627–1632. https://doi.org/10.1111/j.1476-5381.1996.tb15584.x (1996).
17. Hashitani, H. & Edwards, F. R. Spontaneous and neurally activated depolarizations in smooth muscle cells of the guinea-pig urethra. *J. Physiol.* **514** (Pt 2), 459–470. https://doi.org/10.1111/j.1469-7793.1999.459ae.x (1999).
18. Sergeant, G. P., Thornbury, K. D., McHale, N. G. & Hollywood, M. A. Characterization of norepinephrine-evoked inward currents in interstitial cells isolated from the rabbit urethra. *Am. J. Physiol. Cell. Physiol.* **283**, C885–894. https://doi.org/10.1152/ajpcell.00085.2002 (2002).
19. Hollywood, M. A., Sergeant, G. P., McHale, N. G. & Thornbury, K. D. Activation of Ca2+-activated Cl- current by depolarizing steps in rabbit urethral interstitial cells. *Am. J. Physiol. Cell Physiol.* **285**, C327–333. https://doi.org/10.1152/ajpcell.00413.2002 (2003).
20. Sergeant, G. P., Hollywood, M. A., McCloskey, K. D., Thornbury, K. D. & McHale, N. G. Specialised pacemaking cells in the rabbit urethra. *J. Physiol.* **526**, 359–366. https://doi.org/10.1111/j.1469-7793.2000.t01-2-00359.x (2000).
21. Hwang, S. J. et al. Expression of Anoctamin 1/TMEM16A by interstitial cells of Cajal is fundamental for slow wave activity in Gastrointestinal muscles. *J. Physiol.* **587**, 4887–4904. https://doi.org/10.1113/jphysiol.2009.176198 (2009).
22. Gomez-Pinilla, P. J. et al. Ano1 is a selective marker of interstitial cells of Cajal in the human and mouse Gastrointestinal tract. *Am. J. Physiol. Gastrointest. Liver. Physiol.* **296**, G1370–G1381. https://doi.org/10.1152/ajpgi.00074.2009 (2009).
23. Lyons, A. D., Gardiner, T. A. & McCloskey, K. D. Kit-positive interstitial cells in the rabbit urethra: structural relationships with nerves and smooth muscle. *BJU Int.* **99**, 687–694. https://doi.org/10.1111/j.1464-410X.2006.06617.x (2007).
24. McHale, N. G. et al. Organization and function of ICC in the urinary tract. *J. Physiol.* **576**, 689–694. https://doi.org/10.1113/jphysiol.2006.116657 (2006).
25. Gupta, N. et al. Interstitial cell of Cajal-like cells (ICC-LC) exhibit dynamic spontaneous activity but are not functionally innervated in mouse urethra. *Cell. Calcium*. **123**, 102931. https://doi.org/10.1016/j.ceca.2024.102931 (2024).
26. Boedtkjer, D. M. B., Kim, S., Jensen, A. B., Matchkov, V. M. & Andersson, K. E. New selective inhibitors of calcium-activated chloride channels - T16Ainh-A01, CaCCinhA01 and MONNA - What do they inhibit? *Br. J. Pharmacol.* **172**, 4158–4171. https://doi.org/10.1111/bph.13201 (2015).
27. Genovese, M. et al. Analysis of inhibitors of the anoctamin-1 chloride channel (transmembrane member 16A, TMEM16A) reveals indirect mechanisms involving alterations in calcium signalling. *Br. J. Pharmacol.* **180**, 775–785. https://doi.org/10.1111/bph.15995 (2023).
28. Dwivedi, R. et al. The TMEM16A blockers benzbromarone and MONNA cause intracellular Ca(2+)-release in mouse bronchial smooth muscle cells. *Eur. J. Pharmacol.* **947**, 175677. https://doi.org/10.1016/j.ejphar.2023.175677 (2023).
29. Seo, Y. et al. Ani9, a novel potent small-molecule ANO1 inhibitor with negligible effect on ANO2. *PLoS ONE*. **11** https://doi.org/10.1371/journal.pone.0155771 (2016).
30. Lim, X. R., Drumm, B. T., Sergeant, G. P., Hollywood, M. A. & Thornbury, K. D. Ca(2+) -activated Cl(-) channels (TMEM16A) underlie spontaneous electrical activity in isolated mouse corpus cavernosum smooth muscle cells. *Physiol. Rep.* **10**, e15504. https://doi.org/10.14814/phy2.15504 (2022).
31. Drumm, B. T. et al. Ca(2+) signalling in interstitial cells of Cajal contributes to generation and maintenance of tone in mouse and monkey lower oesophageal sphincters. *J. Physiol.* **600**, 2613–2636. https://doi.org/10.1113/jp282570 (2022).
32. Koh, S. D. et al. Propulsive colonic contractions are mediated by inhibition-driven poststimulus responses that originate in interstitial cells of Cajal. *Proc. Natl. Acad. Sci. U S A*. **119**, e2123020119. https://doi.org/10.1073/pnas.2123020119 (2022).
33. Drumm, B. T., Hwang, S. J., Baker, S. A., Ward, S. M. & Sanders, K. M. Ca2 + signalling behaviours of intramuscular interstitial cells of Cajal in the murine colon. *J. Physiol.* **597**, 3587–3617. https://doi.org/10.1113/JP278036 (2019).
34. Koh, S. D. et al. Integrated responses of the SIP syncytium generate a major motility pattern in the colon. *J. Physiol.* https://doi.org/10.1113/jp287315 (2024).
35. Drumm, B. T., Hennig, G. W., Baker, S. A. & Sanders, K. M. Applications of spatio-temporal mapping and particle analysis techniques to quantify intracellular Ca 2 + signaling in situ. *Journal of Visualized Experiments* 1–13, (2019). https://doi.org/10.3791/58989 (2019).
36. Drumm, B. T. et al. Ca2 + signalling in mouse urethral smooth muscle in situ: role of Ca2 + stores and Ca2 + influx mechanisms. *J. Physiol.* **596**, 1433–1466. https://doi.org/10.1113/JP275719 (2018).

37. Rembetski, B. E., Cobine, C. A. & Drumm, B. T. Laboratory practical to study the differential innervation pathways of urinary tract smooth muscle. *Adv. Physiol. Educ.* **42**, 295–304. https://doi.org/10.1152/ADVAN.00014.2018 (2018).
38. Hamill, O. P., Marty, A., Neher, E., Sakmann, B. & Sigworth, F. J. Improved patch-clamp techniques for high-resolution current recording from cells and cell-free membrane patches. *Pflugers Arch.* **391**, 85–100. https://doi.org/10.1007/bf00656997 (1981).
39. Kudo, W., Mitsui, R. & Hashitani, H. Involvement of ANO1 currents in pacemaking of PDGFRα-positive specialised smooth muscle cells in rat caudal epididymis. *Cell. Tissue Res.* **397**, 1–12. https://doi.org/10.1007/s00441-024-03890-x (2024).
40. Grainger, N. et al. Identification and classification of interstitial cells in the mouse renal pelvis. *J. Physiol.* **598**, 3283–3307. https://doi.org/10.1113/JP278888 (2020).
41. Drumm, B. T., Gupta, N., Mircea, A. & Griffin, C. S. Cells and ionic conductances contributing to spontaneous activity in bladder and urethral smooth muscle. *J. Physiol.* https://doi.org/10.1113/jp284744 (2024).
42. Drumm, B. T., Rembetski, B. E., Baker, S. A. & Sanders, K. M. Tonic Inhibition of murine proximal colon is due to nitrergic suppression of Ca 2 + signaling in interstitial cells of Cajal. *Sci. Rep.* **9**, 1–14. https://doi.org/10.1038/s41598-019-39729-7 (2019).
43. Alexandre, E. C. et al. How important is the α < sub > 1 -adrenoceptor in primate and rodent proximal urethra? Sex differences in the contribution of α < sub > 1 -adrenoceptor to urethral contractility. *Am. J. Physiol. - Ren. Physiol.* **312**, F1026–F1034. https://doi.org/10.1152/ajprenal.00013.2017 (2017).
44. Nemenoff, R. A. Vasopressin signaling pathways in vascular smooth muscle. *Front. Biosci.* **3**, d194–207. https://doi.org/10.2741/a274 (1998).
45. Sergeant, G. P., Hollywood, M. A. & Thornbury, K. D. Vol. 1124 (eds (eds Hashitani, H. & Lang, R. J.) 149–167 (Springer Singapore, (2019).
46. Zhu, M. H. et al. A Ca2+-activated Cl- conductance in interstitial cells of Cajal linked to slow wave currents and pacemaker activity. *J. Physiol.* **587**, 4905–4918. https://doi.org/10.1113/jphysiol.2009.176206 (2009).
47. Sanders, K. M., Santana, L. F. & Baker, S. A. Interstitial cells of Cajal - pacemakers of the Gastrointestinal tract. *J. Physiol.* https://doi.org/10.1113/jp284745 (2023).
48. Chen, D. et al. ANO1 in urethral SMCs contributes to sex differences in urethral spontaneous tone. *Am. J. Physiol. Ren. Physiol.* **319**, F394–f402. https://doi.org/10.1152/ajprenal.00174.2020 (2020).
49. Chen, D. et al. Hypertriglyceridemia impairs urethral spontaneous tone through Down-regulation of ANO1 in mouse urethral smooth muscle cells. *Urology* **165**, 157–163. https://doi.org/10.1016/j.urology.2022.01.042 (2022).
50. Feng, M. et al. The RyR-Cl(Ca) -VDCC axis contributes to spontaneous tone in urethral smooth muscle. *J. Cell. Physiol.* **234**, 23256–23267. https://doi.org/10.1002/jcp.28892 (2019).
51. Cruickshank, S. F., Baxter, L. M. & Drummond, R. M. The Cl(-) channel blocker Niflumic acid releases Ca(2+) from an intracellular store in rat pulmonary artery smooth muscle cells. *Br. J. Pharmacol.* **140**, 1442–1450. https://doi.org/10.1038/sj.bjp.0705571 (2003).
52. Balderas, E., Ateaga-Tlecuitl, R., Rivera, M., Gomora, J. C. & Darszon, A. Niflumic acid blocks native and Recombinant T-type channels. *J. Cell. Physiol.* **227**, 2542–2555. https://doi.org/10.1002/jcp.22992 (2012).
53. Oba, T. Niflumic acid differentially modulates two types of skeletal ryanodine-sensitive Ca(2+)-release channels. *Am. J. Physiol.* **273**, C1588–1595. https://doi.org/10.1152/ajpcell.1997.273.5.C1588 (1997).
54. Ottolia, M. & Toro, L. Potentiation of large conductance KCa channels by Niflumic, flufenamic, and mefenamic acids. *Biophys. J.* **67**, 2272–2279. https://doi.org/10.1016/s0006-3495(94)80712-x (1994).
55. Rembetski, B. E., Sanders, K. M. & Drumm, B. T. Contribution of Cav1.2 Ca2 + channels and store-operated Ca2 + entry to pig urethral smooth muscle contraction. *Am. J. Physiol. Ren. Physiol.* **318**, F496–F505. https://doi.org/10.1152/ajprenal.00514.2019 (2020).
56. Wang, P. et al. Inflammatory mediators mediate airway smooth muscle contraction through a G protein-coupled receptor-transmembrane protein 16A-voltage-dependent Ca(2+) channel axis and contribute to bronchial hyperresponsiveness in asthma. *J. Allergy Clin. Immunol.* **141** (e1211), 1259–1268. https://doi.org/10.1016/j.jaci.2017.05.053 (2018).
57. Ghosh, S. et al. Role of voltage-gated Ca(2+) channels and Ano1 Ca(2+)-activated Cl(-) channels in M2 muscarinic receptor-dependent contractions of murine airway smooth muscle. *Am. J. Physiol. Lung Cell. Mol. Physiol.* https://doi.org/10.1152/ajplung.00188.2024 (2025).
58. Alkawadri, T. et al. Contribution of postjunctional M2 muscarinic receptors to cholinergic Nerve-Mediated contractions of murine airway smooth muscle. *Function (Oxf).* **3**, zqab053. https://doi.org/10.1093/function/zqab053 (2022).
59. Wang, M. et al. Downregulation of TMEM16A calcium-activated chloride channel contributes to cerebrovascular remodeling during hypertension by promoting Basilar smooth muscle cell proliferation. *Circulation* **125**, 697–707. https://doi.org/10.1161/circulationaha.111.041806 (2012).

Acknowledgements

The authors would like to thank Alison Bartlett for assistance with breeding and administration of mice at UNR and Dr. Peter Blair at UNR for assistance with immunohistochemical experiments and analysis. We wish to thank Ms Billie McIlveen for animal handling and care at DkIT.

Author contributions

NG: Performed and analyzed qPCR, isometric tension, Ca^{2+} imaging and immunolabelling experiments, co-wrote the manuscript and edited final version for accuracy and intellectual content. S.A.B: Provided resources for and contributed to performing immunolabelling experiments, contributed to data interpretation, manuscript editing and reviewed manuscript for intellectual content. K.M.S: Provided resources for and contributed to performing immunolabelling experiments, contributed to data interpretation, manuscript editing and reviewed manuscript for intellectual content. C.S.G: Contributed to development of hypothesis and supervised research, contributed to development and analysis of qPCR data, contributed to data interpretation, edited manuscript, and reviewed for intellectual content. K.E.R: Performed and analyzed electrophysiological experiments, contributed to development and analysis of qPCR experiments, contributed to writing results section, edited, and reviewed manuscript for intellectual content. D.KF.T: Performed isometric tension experiments, reviewed manuscript for intellectual content. T.A: Performed and analyzed electrophysiological experiments, reviewed manuscript for intellectual content. M.A.H: Contributed to development of hypothesis and supervised research, provided resources for experiments, contributed to data interpretation, edited the manuscript, and reviewed for intellectual content. K.D.T: Contributed to development of hypothesis and supervised research, provided resources for experiments, contributed to data interpretation, edited the manuscript, and reviewed for intellectual content. G.P.S: Contributed to development of hypothesis and supervised research, provided resources for experiments, contributed to data interpretation, edited the manuscript, and reviewed for intellectual content. B.T.D: Conceived of research project, developed hypothesis, supervised research, provided resources for experiments, wrote original draft of manuscript, contributed to data interpretation, edited the manuscript, and

reviewed for intellectual content. All authors read and approved the manuscript before submission. All persons designated as authors qualify for authorship, and all those who qualify for authorship are listed. All authors agree to be accountable for all aspects of the work in ensuring that questions related to the accuracy or integrity of any part of the work are appropriately investigated and resolved.

Funding
This work was supported by funding from the Irish Higher Education Authority Technological University Transformation Fund TUTFY2144 (to BTD), Government of Ireland - European Union Regional Development Framework - TU RISE CREATE-DkIT Scholarship CREAT-PhD-4 (BTD), a Physiological Society Early Career Grant (BTD) and R01 DK124509 (KMS) & R01 DK119491 (KMS) from the National Institutes of Health (USA).

Declarations

Competing interests
The authors declare no competing interests.

Additional information
Correspondence and requests for materials should be addressed to B.T.D.

Reprints and permissions information is available at www.nature.com/reprints.

Publisher's note Springer Nature remains neutral with regard to jurisdictional claims in published maps and institutional affiliations.